

## DECOMPOSITION OF SULFUR HEXAFLUORIDE BY X-RAYS

J. K. Olthoff and R. J. Van Brunt

Electricity Division  
National Institute of Standards and Technology\*  
Gaithersburg, Maryland 20899

### INTRODUCTION

The decomposition of gaseous sulfur hexafluoride ( $\text{SF}_6$ ) by exposure to high-energy photons, and the subsequent formation of toxic and corrosive oxyfluoride by-products, is of interest due to the use of  $\text{SF}_6$  as a high-voltage insulator near sources of radiation, such as particle accelerators and X-ray units. Additionally, information about by-product formation due to radiation exposure can be compared with data obtained for the decomposition of  $\text{SF}_6$  in electrical discharges.<sup>1,2</sup> This comparison is interesting since the volume in which the decomposition occurs is usually many orders of magnitude larger for radiation exposure than for electrical discharges. However, little previous work has been done to determine the effects of radiation upon gaseous  $\text{SF}_6$ .<sup>3</sup>

In this paper, we present results of by-product formation in gaseous  $\text{SF}_6$  exposed to high-energy X-rays. The identity and concentration of the decomposition by-products are determined by gas chromatography/mass spectrometry techniques that were developed to investigate the decomposition of  $\text{SF}_6$  exposed to corona discharges.<sup>1,4</sup> The production curves of  $\text{SOF}_2$  and  $\text{S}_2\text{F}_{10}$  are determined for a range of  $\text{SF}_6$  gas pressures, X-ray energies, and X-ray fluxes. Evidence for the presence of other by-products, such as  $\text{SOF}_4$ ,  $\text{SO}_2\text{F}_2$ , and  $\text{S}_2\text{O}_2\text{F}_{10}$  is also presented. The decomposition data for the  $\text{SF}_6$  exposed to X-rays are compared with previously published data for  $\text{SF}_6$  exposed to corona discharges.

### EXPERIMENTAL DESCRIPTION

The beam of high-energy X-rays used to irradiate samples of  $\text{SF}_6$  was produced by a commercial X-ray unit. X-rays were generated in the unit by a high-energy beam of electrons striking a tungsten surface at a  $20^\circ$  incident angle. The energy and intensity of the X-rays were varied by changing the accelerating voltage ( $V_x$ ) and current ( $I_x$ ) of the incident electron beam. For the experiments presented here, electron energies of 100 kV and 195 kV were used, with electron currents of 4.0, 2.5, and 1.0 mA. The X-rays then pass through approximately 1 mm of glass and 4 mm of aluminum before exiting the X-ray unit.

\*Electronics and Electrical Engineering Laboratory, Technology Administration, U. S. Department of Commerce

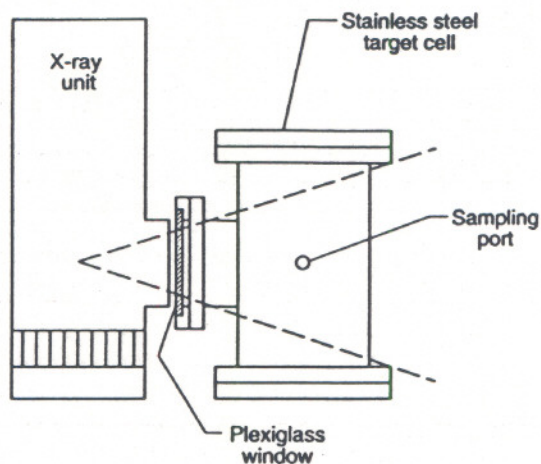


Figure 1. Schematic diagram of the apparatus used to investigate the decomposition of SF<sub>6</sub> by exposure to X-rays. The dashed lines show the approximate spatial spread of the X-ray beam.

The SF<sub>6</sub> that was exposed to the X-ray beam was contained in a stainless steel vacuum chamber with a volume of 6.2 l. Prior to filling with SF<sub>6</sub>, the vacuum chamber was evacuated by a mechanical vacuum pump down to approximately 1 Pa, and then flushed several times with SF<sub>6</sub>. During the experiments, the gas pressures in the cell were maintained at 300 or 600 kPa. The vacuum chamber was equipped with a 10-mm-thick, 100-mm-diameter plexiglass window, through which the X-rays were directed, and a sampling port that allowed the sampling of the compressed SF<sub>6</sub> from inside of the cell by a gas-tight syringe through a rubber septum. The X-ray unit and target cell were placed in a lead-lined concrete bunker, with the two chambers sufficiently close together such that the entire X-ray beam intercepted the target cell. This arrangement is shown schematically in Fig. 1.

To determine the effects of irradiation by X-rays on an SF<sub>6</sub> sample, the X-ray unit was operated for a set period of time at a particular beam current and voltage setting. During the experiment, the X-ray unit was periodically turned off, and the target cell was removed from the radiation bunker for gas analysis. The gas was analyzed using gas chromatography/mass spectrometry (GC/MS) techniques that are described in detail elsewhere.<sup>1,4</sup> In brief, 0.5 ml samples of decomposed SF<sub>6</sub> were removed from the target cell by gas-tight syringe. The samples were then injected into the GC/MS where the various components of the gas are separated in time as the gas flows through the chromatographic column. The compounds SOF<sub>2</sub>, SO<sub>2</sub>F<sub>2</sub>, and SOF<sub>4</sub> were detected using a Poropak<sup>1</sup> column in the GC, whereas detection of S<sub>2</sub>F<sub>10</sub> and S<sub>2</sub>O<sub>2</sub>F<sub>10</sub> requires use of a Chromosorb<sup>1</sup> column. Both columns were operated at room temperature with helium carrier gas. The various compounds were then detected by monitoring ions created by electron impact in the source of a mass spectrometer. For example, ion 80 (SOF<sub>2</sub><sup>+</sup>) was monitored to detect SOF<sub>2</sub> and SOF<sub>4</sub>, and ion 83 (SO<sub>2</sub>F<sup>+</sup>) was observed to detect SO<sub>2</sub>F<sub>2</sub>. Ion 86 was also used to detect S<sub>2</sub>F<sub>10</sub> due to a conversion of S<sub>2</sub>F<sub>10</sub> to SOF<sub>2</sub> that occurs at the heated interface between the GC column and the mass spectrometer.<sup>4</sup>

<sup>1</sup>Certain commercial equipment, instruments, or materials are identified in this paper to specify adequately the experimental procedure. Such identification does not imply recommendation or endorsement by the National Institute of Standards and Technology, nor does it imply that the material or equipment identified are necessarily the best available for the purpose.

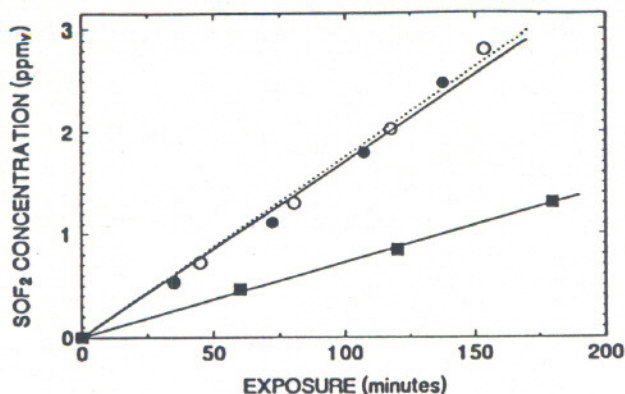


Figure 2. Production curves for  $\text{SOF}_2$  in a  $\text{SF}_6$  sample exposed to X-rays. The X-ray voltage and  $\text{SF}_6$  gas pressures used to obtain these data are: (●)  $V_x = 195$  kV,  $P = 600$  kPa; (■)  $V_x = 100$  kV,  $P = 600$  kPa; (○)  $V_x = 195$  kV,  $P = 300$  kPa. The beam current ( $I_x$ ) of the X-ray unit was 2.5 mA for all data in this figure. The solid lines are the least square fit for the 600 kPa data, while the dotted line is the least square fit for the 300 kPa data.

To calibrate the response of the GC/MS to the presence of the decomposition products, injections from reference samples containing known concentrations of  $\text{SOF}_2$ ,  $\text{SO}_2\text{F}_2$ ,  $\text{SOF}_4$ , or  $\text{S}_2\text{F}_{10}$  were made immediately before and after injections from the target cell. Uncertainties in the relative concentrations of by-products in the target cell due to variations in injection sizes and changes in GC/MS sensitivity were calculated to be less than  $\pm 4\%$ . However, the absolute concentrations of oxyfluorides in the prepared reference samples used to calibrate the GC/MS were observed to vary by as much as  $\pm 25\%$ , which significantly increases the uncertainties of the measured production rates.

## RESULTS

The GC/MS analysis of the  $\text{SF}_6$  exposed to the X-ray beam indicates that  $\text{SOF}_2$  is probably the primary gas-phase decomposition product from the interaction of the radiation with the gas. Figure 2 shows the production curves (solid lines) for  $\text{SOF}_2$  inside the cell for  $V_x = 195$  kV and 100 kV, with  $I_x = 2.5$  mA and a  $\text{SF}_6$  pressure of 600 kPa. The  $\text{SOF}_2$  concentrations are given in parts in  $10^6$  by volume ( $\text{ppm}_v$ ). A clear voltage dependence is observed indicating that the production rate is dependent upon the energy of the irradiating X-rays. The production curve represented by open circles and a dotted line in Fig. 2 is for an  $\text{SF}_6$  pressure of 300 kPa with  $I_x = 2.5$  mA and  $V_x = 195$  kV. The agreement between this data and the data obtained at 600 kPa, clearly shows that the production rate of  $\text{SOF}_2$  by exposure to X-rays is not dependent upon the  $\text{SF}_6$  gas pressure.

Figure 3 illustrates the dependence of  $\text{SOF}_2$  production upon the intensity of the X-ray beam, by showing the production curves for different setting of  $I_x$  with  $V_x$  held constant at 195 kV. As expected, the production rate of  $\text{SOF}_2$  increases with increasing  $I_x$ , corresponding to higher X-ray beam intensities. However, the observed dependence does not scale linearly with  $I_x$ .

Production of  $\text{SO}_2\text{F}_2$  and  $\text{SOF}_4$  was also observed for all of the experimental conditions investigated. Unfortunately,  $\text{SOF}_4$  and  $\text{SO}_2\text{F}_2$  have nearly the same GC retention times which results in significant signal interference if both are present in the gas sample.<sup>1</sup> Therefore, production rates for  $\text{SO}_2\text{F}_2$  and  $\text{SOF}_4$  inside the target cell could

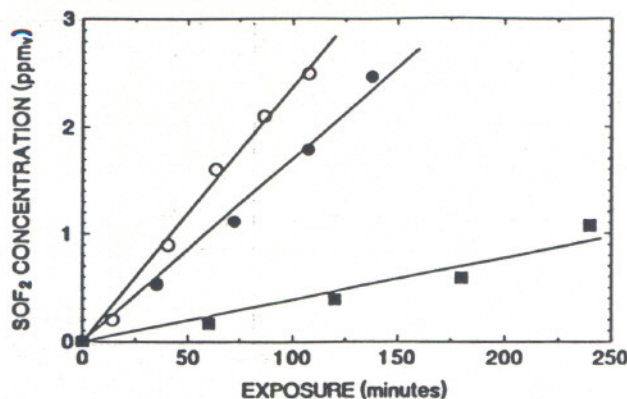


Figure 3. SOF<sub>2</sub> production curves for 600-kPa SF<sub>6</sub> samples decomposed by exposure to X-rays produced with V<sub>x</sub> = 195 kV and (■) I<sub>x</sub> = 1.0 mA, (●) I<sub>x</sub> = 2.5 mA, and (○) I<sub>x</sub> = 4.0 mA.

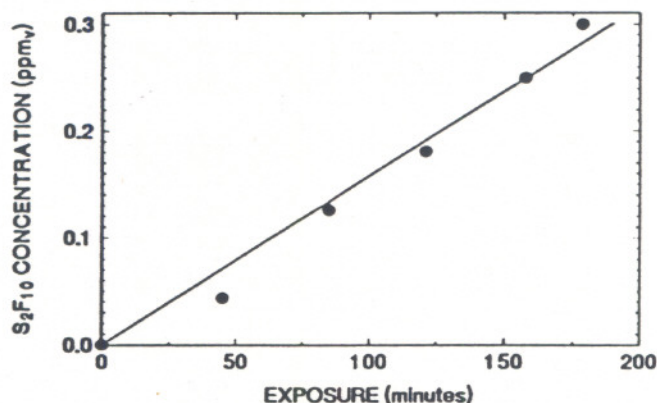


Figure 4. Production curve for S<sub>2</sub>F<sub>10</sub> formed in a 300-kPa SF<sub>6</sub> sample exposed to X-rays produced with V<sub>x</sub> = 195 kV and I<sub>x</sub> = 2.5 mA.

not be determined. However, the magnitude of the combined signal observed in these experiments does not preclude the possibility that concentrations of SO<sub>2</sub>F<sub>2</sub> and SOF<sub>4</sub> in the decomposed SF<sub>6</sub> may be of the same order as those measured for SOF<sub>2</sub>.

Production of S<sub>2</sub>F<sub>10</sub> and S<sub>2</sub>O<sub>2</sub>F<sub>10</sub> was also observed in the target cell, and a production curve for S<sub>2</sub>F<sub>10</sub> is shown in Fig. 4 for a 300-kPa SF<sub>6</sub> sample irradiated by the X-ray beam with V<sub>x</sub> = 195 kV and I<sub>x</sub> = 2.5 mA. The production rates of S<sub>2</sub>F<sub>10</sub> are nearly a factor of ten lower than those observed for SOF<sub>2</sub>. No quantitative analysis was performed for S<sub>2</sub>O<sub>2</sub>F<sub>10</sub> due to the lack of a reliable reference sample.

## DISCUSSION AND CONCLUSIONS

The by-products produced in SF<sub>6</sub> during exposure to X-rays are essentially the same as the by-products produced by corona,<sup>1,2</sup> sparks,<sup>5</sup> and arcs<sup>6</sup> in SF<sub>6</sub>. This implies that the chemistry of by-product formation in decomposed SF<sub>6</sub> is essentially independent of the dissociation mechanism. Interestingly, the relative production rates of S<sub>2</sub>F<sub>10</sub> and SOF<sub>2</sub> for dissociation of SF<sub>6</sub> by X-rays are nearly the same as for cases where SF<sub>6</sub> is decomposed by exposure to corona discharges.<sup>1,2</sup> This implies that the SF<sub>5</sub> radical, the precursor to S<sub>2</sub>F<sub>10</sub> formation, must possess a relatively long lifetime under the conditions used here, because of the large volume in which S<sub>2</sub>F<sub>10</sub> formation occurs during

exposure to radiation (a factor of  $10^9$  larger than in a corona discharge).<sup>7</sup> The data also show that a significant concentration of toxic by-products can be produced by X-ray exposure in a relatively short period of time (hundreds of minutes). This fact should be taken into account when dealing with the safe handling of SF<sub>6</sub> that has been exposed to radiation.

The dissociation of SF<sub>6</sub> in the presence of X-rays may be caused by either of two processes: (1) direct photodissociation of the gas by K-shell absorption by the sulfur and the fluorine, or (2) dissociation or dissociative attachment induced by secondary electrons generated by X-rays striking the back wall of the target cell. Direct photodissociation of SF<sub>6</sub> is due to K-shell absorption by the sulfur and fluorine, with absorption edges at 2.3 keV and 0.68 keV, respectively.<sup>8</sup> Dissociative attachment is due to the capture of a free electron to form a temporary negative ion that dissociates into a stable negative ion and a neutral fragment.<sup>9</sup>

The fact that the concentration of decomposition by-products in the target cell is independent of pressure (see Fig. 2) suggests that the primary dissociating process under these conditions is photodissociation, since the number of secondary electrons produced by the X-rays will not change significantly with gas pressure. In order to verify this conclusion, a curved, perforated stainless steel plate was installed inside the target cell, 2 mm from the back wall of the chamber. A dc voltage (20 kV) was then applied to the plate in order to produce an electric field inside the target gas while the sample was exposed to the X-ray source. Since the dissociation or dissociative attachment processes are highly dependent upon the energy of the free electrons, the rate of by-product formation would vary with the applied electric field if these processes played a significant role in SF<sub>6</sub> dissociation. However, the production rates of the decomposition by-products were observed to be unaffected by the applied field, thus indicating that secondary electrons do not play a major role in the dissociation of SF<sub>6</sub> under these conditions. This confirms that photodissociation is the primary means of decomposition of SF<sub>6</sub> in the presence of high-energy photons.

## REFERENCES

1. R. J. Van Brunt, Production rates for oxyfluorides SOF<sub>2</sub>, SO<sub>2</sub>F<sub>2</sub>, and SOF<sub>4</sub> in SF<sub>6</sub> corona discharges, *J. Res. Natl. Burcau Standards*, 90:229 (1985).
2. R. J. Van Brunt, J. K. Olthoff, and M. Shah, Rate of S<sub>2</sub>F<sub>10</sub> production from negative corona in compressed SF<sub>6</sub>, in: "Conference Record of the 1992 IEEE Symposium on Electrical Insulation," IEEE, Piscataway, NJ (1992).
3. R. Hergli, J. Casanovas, A. Derdouri, R. Grob, and J. Mathieu, Study of the decomposition of SF<sub>6</sub> in the presence of water, subjected to gamma radiation or corona discharges, *IEEE Trans. Electrical Insul.* 23:451 (1988).
4. J. K. Olthoff, R. J. Van Brunt, J. T. Herron, and I. Sauers, Detection of trace disulfur decafluoride in sulfur hexafluoride by gas chromatography/mass spectrometry, *Anal. Chem.* 63:726 (1991).
5. I. Sauers, By-product formation in spark breakdown of SF<sub>6</sub>/O<sub>2</sub> Mixtures, *Plasma Chem. Plasma Process.* 8:247 (1988).
6. B. Belmadani, J. Casanovas, A. M. Casanovas, R. Grob, and J. Mathieu, SF<sub>6</sub> decomposition under power arcs, *IEEE Trans. Electrical Insul.* 26:1163 (1991).
7. R. J. Van Brunt and J. T. Herron, Plasma chemical model for decomposition of SF<sub>6</sub> in a negative glow discharge, in preparation.
8. CRC Handbook of Chemistry and Physics, R. C. Weast, Ed., CRC Press, Boca Raton, FL (1986).
9. H.-X. Wan, J. H. Moore, J. K. Olthoff, and R. J. Van Brunt, Electron scattering and dissociative attachment by SF<sub>6</sub> and its electrical-discharge by-products, *Plasma Chem. Plasma Process.* 13:1 (1993).

## DISCUSSION

**J. CASTONGUAY:** Can you comment on the reaction schemes that produce a similar relative ratio of  $S_2F_{10}/SO_2$  in your "diffused" reaction volume compared to the "minute" and very localized corona discharges?

**J. OLTHOFF:** The fragmentations of  $SF_6$  by X-rays and by corona both produce  $SF_5$  radicals. The surprising aspect of  $S_2F_{10}$  formation in the large volume exposed to X-rays, is that the  $SF_5$  radicals exist long enough to find each other and form  $S_2F_{10}$ .